BEAM TESTS OF DIAMOND-LIKE CARBON COATING FOR MITIGATION OF ELECTRON CLOUD

J. Eldred, M. Backfish, C.Y. Tan, R. Zwaska, FNAL, Batavia, IL 60510, USA
S. Kato, KEK, Tsukuba, Ibaraki 305-0801, Japan

Abstract

Electron cloud beam instabilities are an important consideration in virtually all high-energy particle accelerators and could pose a formidable challenge to forthcoming high-intensity accelerator upgrades. Our results evaluate the efficacy of a diamond-like carbon (DLC) coating for the mitigation of electron in the Fermilab Main Injector. The interior surface of the beampipe conditions in response to electron bombardment from the electron cloud and we track the change in electron cloud flux over time in the DLC coated beampipe and uncoated stainless steel beampipe. The electron flux is measured by retarding field analyzers placed in a field-free region of the Main Injector. We find the DLC coating reduces the electron cloud signal to roughly 2% of that measured in the uncoated stainless steel beampipe.

BACKGROUND

Electron cloud instabilities have been observed in a variety of modern proton accelerators [1–5] including a recent instability encountered in the Fermilab Recycler [6].

During the build-up of electron cloud, the particle beam causes the transverse acceleration of stray electrons which then scatter additional electrons from the beampipe. The number of electrons increase exponentially until a saturation is reached. The secondary electron yield (SEY) of a surface is the ratio of the average number of electrons scattered from the surface to the number of electron impacting the surface. The density of the electron cloud depends critically on beam intensity and SEY of the inner surface of the beampipe.

One promising way to reduce electron cloud formation is to coat the inside of the beampipe with low-SEY materials. In this work we test the performance of a diamond-like carbon (DLC) coating for mitigation of electron cloud in the Fermilab Main Injector. DLC coatings have been tested for electron cloud mitigation first at KEKB LER [7] and CERN SPS [8]. The KEKB group prepared the DLC coated beampipe for this work and the SEY of the DLC is directly measured in [9]. The first in-situ SEY measurements were conducted at KEKB in 2007 [10].

To properly characterize the electron cloud mitigation performance of the materials, the electron flux needs to be studied over time. Conditioning is the process where the bombarding electrons change the surface chemistry of the beampipe (see [11–13]). As the beampipe conditions its secondary electron yield lowers and a greater beam intensity would be required to generate the same electron cloud flux.

Table 1 indicates the Main Injector parameters used for our results. Simulations of electron cloud buildup in the Fermilab Main Injector can be found in [14].

Table 1: Main Injector Parameters

Energy	8–120 GeV
Circumference	3319.4 m
RF frequency	52.8–53.1 MHz
Beam Intensity	$35–50 \times 10^{12}$ protons
Bunch Intensity	12×10^{10} protons
Bunch Spacing	18.9 ns
Bunch Length	1–10 ns @ 95%
Beam Admittance	40π mm·mrad
Beam Emittance	15π mm·mrad
Beampipe Inner Diameter	149.2 mm

MI-52 BEAMPIPE TEST STATION

The beampipe test station at MI-52, shown in Figure 1, was installed to measure the performance of beampipe coatings for the mitigation of electron cloud [15, 16]. The MI-52 test station uses electron cloud detectors, called retarding field analyzers (RFAs) [17, 18], to compare the performance of uncoated and coated beampipe. RFA1 is located at the center of an uncoated stainless steel (SS) section and RFA3 is located in the center of a coated beampipe section. RFA2 and RFA4 are not used for this study.

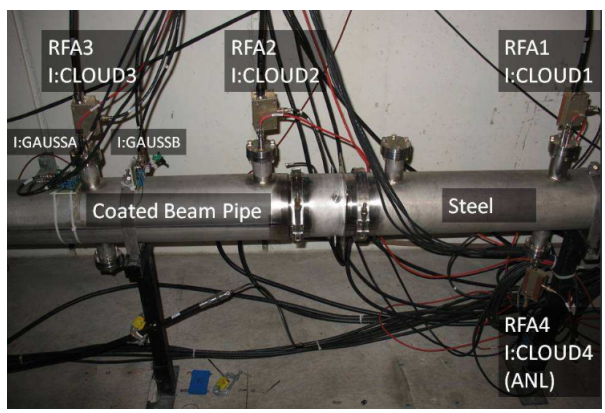

Figure 1: The electron cloud measurement setup in the Main Injector at MI-52. The setup primarily consists of four RFAs and two beampipe sections. The beampipe is 6" in diameter and the coated and uncoated sections are each ∼1 meter long. The setup is located in a straight section to avoid electron confinement from magnets.

Fermilab uses the ACNET control system [19] and our work relies on the Lumberjack Datalogger module [20] to automatically trigger, read, timestamp, and record the electron cloud signal at each RFA. For each RFA location, the

ISBN 978-3-95450-182-3

Datalogger module records the maximum electron cloud signal obtained in each Main Injector ramp cycle [15].

The MI-52 test station was used to measure the performance of titanium nitride and amorphous carbon in 2009 and 2010 [15]. In September 2013, the DLC coated beampipe was installed. Between September 2013 and January 2016 the Fermilab Recycler was being commissioned for higher power operation and during this time the per-pulse intensity was limited [21]. The DLC beampipe did not show any long-term conditioning effect at a beam intensity of 25×10^{12} protons [15]. In this work however we find that the DLC material rapidly conditions at beam intensities above 35×10^{12} protons and strongly mitigates electron cloud at the highest intensities tested in the Main Injector (55×10^{12}). We find that the electron cloud flux in the DLC region is approximately 2% of the electron flux in the SS region. We assess the performance of DLC material to be comparable or superior to the performance of the titanium nitride.

The MI-52 test station was offline from June 2015 to January 2016 due to radiation damage [22]. The RFA preamplifers were progressively damaged during the Main Injector slow-extraction cycle by particles backscattered from the downstream Lambertson magnet. Only two of the preamplifer rad-hard op-amp chips [23] could be replaced, leaving RFA 2 and RFA 4 currently inactive (see Fig. 1). RFA 1 and RFA 3 are now protected by an event-triggered relay box that deactivates the preampliers during the Main Injector slow-extraction cycle.

DLC COATING PERFORMANCE & CONDITIONING

The high-intensity run of the DLC material for mitigation of electron cloud begins in January 2016. Figure 2 shows beam intensity in Main Injector for all regular cycles of the high-intensity DLC run. In Fall 2017 there was a long maintenance shutdown period during which the MI-52 test station was brought up from vacuum. Some low-intensity cycles are excluded from this dataset, because the electron flux at MI-52 test station is only logged during regular Main Injector operation.

In this electron cloud density regime, the electron flux has a quasi-exponential dependence on beam intensity as shown in Fig 3. The beam intensity associated with the onset of electron cloud is itself a product of the SEY of the beampipe material. As the beampipe material conditions, higher intensities are required to generate the same flux of electrons.

In [15], we defined a benchmark beam intensity x_0 to be the beam intensity at which the electron cloud flux is 10^7 electrons per cm^2 per second. This electron flux corresponds to a 1V signal that shows up clearly in the detection range of RFA electron cloud monitors. At this benchmark the electron cloud does not produce any detectable adverse effect on proton beam quality.

For our results in [15], the benchmark beam intensity x_0 at a given point of time was found by an exponential fit of

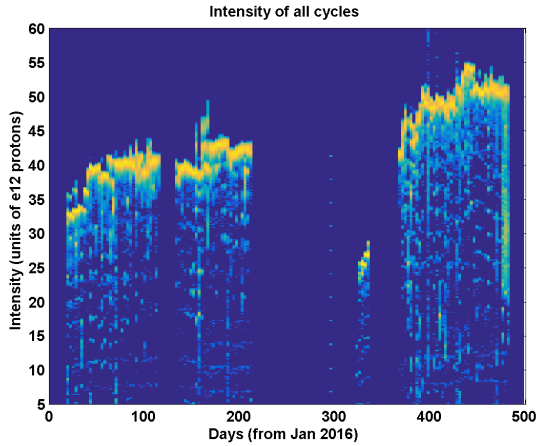

Figure 2: 2D histogram of Main Injector beam intensity over time. The color axis is log-scale.

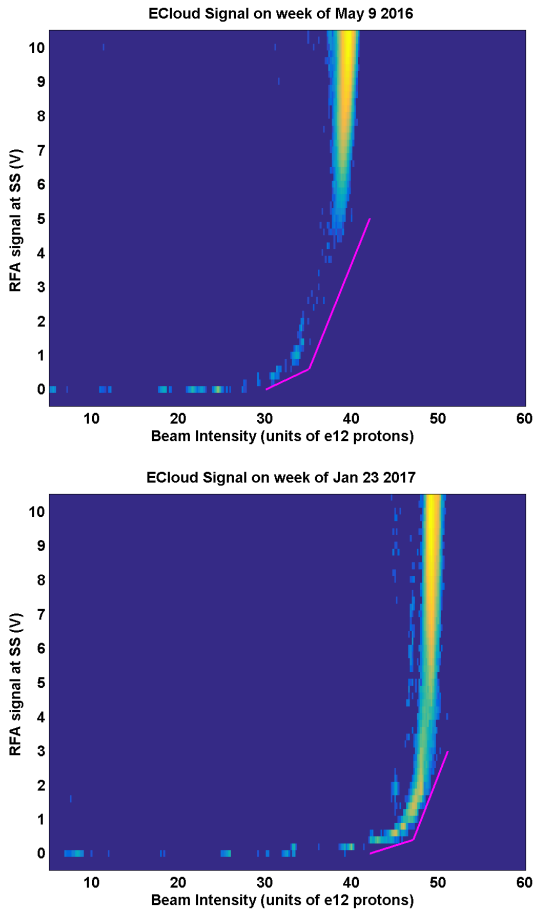

Figure 3: 2D histogram of electron cloud signal and beam intensity at SS location [24]. Conditioning has taken place between week of May 9 2016 (top) and week of Jan 23 2017 (bottom).

ISBN 978-3-95450-182-3

the RFA signal as a function of beam intensity. In this work we use a different method because the beam intensity was inadequately sampled over the fit range.

Figure 4 and Figure 5 show a 2D histogram of the beam intensity and timestamp for all cycles with RFA electron cloud signals between 0.8V and 1.2V at each location. Within each 3-day time bin, the benchmark beam intensity x_0 is taken to be the median beam intensity. If 99.99% of all RFA signals are below 0.8V in a time-bin, we instead take the benchmark beam intensity x_0 to be the maximum beam intensity in that time bin.

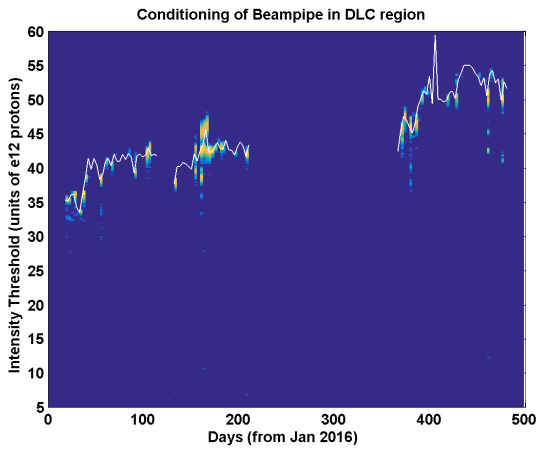

Figure 4: 2D histogram of the beam intensity and timestamp, for cycles with RFA electron cloud signals between 0.8V and 1.2V at the SS location.

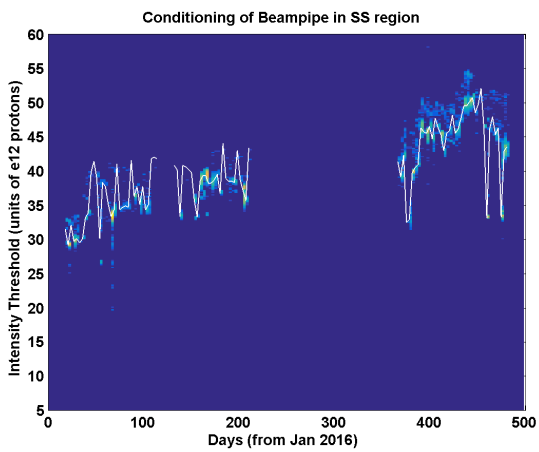

Figure 5: 2D histogram of the beam intensity and timestamp, for cycles with RFA electron cloud signals between 0.8V and 1.2V at the DLC location.

Figure 6 juxtaposes the benchmark intensity for the SS and DLC with the average beam intensity over time. The large fluctuations in the SS benchmark intensity might indicate a sensitivity to other beam parameters such as bunch length, emittance, or beam offset. As the average beam intensity increases, the rate of electron bombardment on the material increases exponentially, and the material conditions rapidly. The DLC conditions as a result of a much smaller electron flux than the SS.

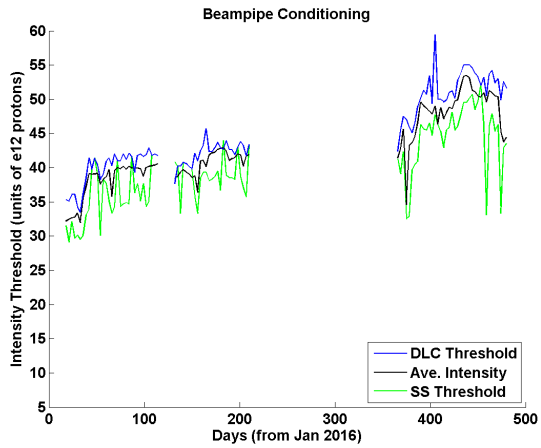

Figure 6: Beam intensity associated with a 1V RFA electron cloud signal at the DLC (blue) and SS (green) locations. Average beam intensity (black) shown for comparison.

CONCLUSION

The MI52 test station allows us to directly compare the electron cloud flux in coated and uncoated sections of beampipe during high-intensity accelerator operation. We track the conditioning of the beampipe materials over time by recording the beam intensity at which a benchmark electron flux is reached. In this intensity regime ($35 - 50 \times 10^{12}$ protons) the DLC material conditions rapidly and reduces electron cloud flux by approximately a factor of 50 relative to SS. We find the performance of the DLC material comparable or superior to the performance of previously tested materials titanium nitride and amorphous carbon [15]. The ultimate performance of a maximally conditioned DLC coated beampipe remains beyond the capabilities of the Main Injector to test at its current beam intensity.

ACKNOWLEDGMENTS

Operated by Fermi Research Alliance, LLC under Contract No. DE-AC02-07CH11359 with the United States Department of Energy.

This work was partially supported with the U.S.-Japan Science and Technology Cooperation Program in High Energy Physics.

REFERENCES

[1] G. Arduini, T. Bohl, K. Cornelis, *et al.*, in *Proc. ECLOUD'04*, [http://mafurman.lbl.gov/ECLOUD04_proceedings/arduini-ga_ecloud04_v2.pdf].

[2] G. Iadarola, H. Bartosik, G. Rumolo, *et al.*, in *Proc. IPAC'14*, [www.jacow.org/IPAC2014/papers/tupme027.pdf].

[3] W. Fischer, M. Blaskiewicz, J. M. Brennan, *et al.*, *Phys. Rev. Lett.*, vol. 11, p. 041002, 2008, [http://journals.aps.org/prstab/pdf/10.1103/PhysRevSTAB.11.041002].

ISBN 978-3-95450-182-3

[4] R. J. Macek, A. Browman, D. Fitzgerald, *et al.*, in *Proc. PAC'01*, [http://accelconf.web.cern.ch/AccelConf/p01/PAPERS/FOAB007.PDF].

[5] M. Blaskiewicz, M. A. Furman, M. Pivi, *et al.*, *Phys. Rev. Lett.*, vol. 6, p. 014203, 2003, [http://journals.aps.org/prstab/pdf/10.1103/PhysRevSTAB.6.014203].

[6] S. A. Antipov, P. Adamson, A. Burov, *et al.*, *Phys. Rev. Lett.*, vol. 20, p. 044401, 2017, [http://journals.aps.org/prab/abstract/10.1103/PhysRevAccelBeams.20.044401].

[7] S. Kato and M. Nishiwaki, in *Proc. ECLOUD'10*, [https://accelconf.web.cern.ch/accelconf/Ecloud2010/papers/mit00.pdf];
M. Nishiwaki and S. Kato, in *Proc. IPAC'10*, [http://accelconf.web.cern.ch/AccelConf/IPAC10/papers/thpea079.pdf]

[8] C. Yin Vallgren, P. Chiggiato, P. Costa Pinto, *et al.*, in *Proc. IPAC'11*, [http://accelconf.web.cern.ch/AccelConf/IPAC2011/papers/TUPS028.PDF].

[9] S. Kato and M. Nishiwaki, presented at AEC'09, [http://indico.cern.ch/event/62873/session/3/contribution/24/material/slides/0.pdf].

[10] S. Kato and M. Nishiwaki, in *Proc. ECLOUD'07*;
M. Nishiwaki and S. Kato, in *Proc. ECLOUD'07*, [http://chep.knu.ac.kr/ecloud07/upload/ECloud07_Proc_v2.pdf].

[11] R. Larciprete, D. R. Grosso, R. Flammini, *et al.*, in *Proc. ECLOUD'12*, [http://cds.cern.ch/record/1567017/files/p99.pdf].

[12] Y. Li, X. Liu, J. Conway, *et al.*, in *Proc. IPAC'13*, [http://accelconf.web.cern.ch/accelconf/ipac2013/papers/thpfi088.pdf].

[13] C. Yin Vallgren, Doctoral dissertation, Chalmers University of Technology, 2011 [http://cds.cern.ch/record/1374938/files/CERN-THESIS-2011-063.pdf?version=2].

[14] P. L. G. Lebrun. P. Spentzouris, J. R. Cary, *et al.*, in *Proc. ECLOUD'10*, [www.jacow.org/ECLOUD2010/papers/MOD03.pdf].

[15] M. Backfish, J. Eldred, C. Y. Tan, *et al.*, *IEEE Trans. Nucl. Sci.*, vol. 63, p. 957, 2016, [http://ieeexplore.ieee.org/document/7305834/].

[16] R. M. Zwaska, in *Proc. PAC'11*, [http://accelconf.web.cern.ch/AccelConf/PAC2011/papers/MOOBS4.PDF].

[17] R. A. Rosenberg and K. C. Harkay, *Nucl. Instrum. Meth. A*, vol. 453, p. 3, 2000, [http://www.sciencedirect.com/science/article/pii/S0168900200004721].

[18] X. Zhang, A. Z. Chen, W. Chou, *et al.*, J.-F. Ostiguy *et al.*, in *Proc. PAC'07*, [http://accelconf.web.cern.ch/AccelConf/p07/PAPERS/THPAN117.PDF].

[19] J. Patrick, Fermilab Report No. Beams-doc-1762, 2005, [https://beamdocs.fnal.gov/AD/DocDB/0017/001762/001/smtf_patrick.ppt].

[20] K. Cahill, Fermilab Report No. Beams-doc-661, 2005, [https://beamdocs.fnal.gov/AD/DocDB/0006/000661/003/DataLogging.pdf].

[21] P. Adamson, in *Proc. HB'16*, [http://accelconf.web.cern.ch/AccelConf/hb2016/papers/tham1x01.pdf].

[22] J. Eldred, Fermilab Report No. Beams-doc-5151, 2016, [https://beamdocs.fnal.gov/AD/DocDB/0051/005151/001/Budker_MI52.ppt].

[23] Intersil Datasheet HS-5104ARH-EH, 2013, [http://www.intersil.com/content/dam/Intersil/documents/hs-5/hs-5104arh-eh.pdf].

[24] The ACNET Datalogger can erroneously pair the beam intensity for a full cycle with the RFA signal for an empty cycle. This artifact has been removed with a simple cut indicated by the magenta line.